Shape change, engulfment, and breakup of partially engulfed compound drops undergoing thermocapillary migration

O. M. Lavrenteva,[1] L. Rosenfeld,[2] and A. Nir[1]
[1]*Chemical Engineering Department, Technion, Haifa IL-32000, Israel*
[2]*Chemical Engineering Department, Stanford University, Stanford, California 94305, USA*
(Received 21 July 2011; published 23 November 2011)

Compound drops comprise two or more immiscible phases, one of which entirely or partially engulfs the others. In this work we consider the thermocapillary-induced motion of partially engulfed compound drops, composed of two phases, in an immiscible fluid. If the capillary number is negligibly small, Ca $\ll 1$, the partially engulfed compound drop is composed of three spherical surface segments, intersecting at contact angles that are determined by the three interfacial tensions associated with the three fluid phases that make up the compound drop and the ambient medium. Corrections to the shapes of the undeformable case at Ca $= 0$ are expected to be of the order Ca. However, as the drop propagates through the nonisothermal fluid, the temperature at the three-phase contact line and, hence, the contact angles, may considerably change, resulting in a dramatic change of the compound drop shape. Moreover, the changes in the interfacial tensions may be so significant that the partially engulfed configuration may become impossible and either two immiscible parts of the compound drop separate or one of them becomes completely engulfed by the other.

DOI: 10.1103/PhysRevE.84.056323 PACS number(s): 47.55.D−, 47.55.pf, 47.15.G−

I. INTRODUCTION

Bulk fluid motion induced by interfacial dynamics has been studied for over a century. One of the most interesting phenomena is the thermocapillary drift of fluid particles through a viscous fluid. The thermocapillary flow is induced by a gradient of the surface tension at the interface as a result of a nonuniform temperature or surfactant distribution in the surrounding media. The surface tension gradient results in a tangential stress on the interface, which causes motion of the surrounding liquid by viscous traction. Then, the submerged droplet or bubble will move in the direction of decreasing interfacial tension, thus decreasing its surface energy.

Young, Goldstein, and Block [1] obtained a theoretical prediction for the migration velocity of a single spherical drop, which is placed in a viscous fluid with an imposed constant temperature gradient, assuming negligible Reynolds, Re; capillary, Ca; and Peclet, Pe, numbers. Later Bratukhin [2] constructed the correction to this solution assuming that all three parameters are proportional to a single small parameter, the Marangoni number. Balasubramaniam and Chai [3] considered Re, Ca, and Pe as independent parameters and showed that the solution constructed in Ref. [1] satisfies the full Navier-Stokes equations in the case of negligible convective transport. This remarkable result is valid, however, solely for a single-phase drop in an unbounded media. The boundary of a drop would deform even at 0 Reynolds and Peclet numbers, if other particles or boundaries are present in the system or when the drop itself consists of two or more immiscible phases, one of which completely or partially engulfs the others. The present study is focused on the latter case of a two-phase partially engulfed compound drop.

Nonhomogeneous temperature or concentration distribution at the interface of a drop may be imposed by distant boundary conditions (the case considered in, e.g., Refs. [1–3]) or it may be caused by heat transfer between the phases in suspension that eventually results in a spontaneous thermocapillary migration of drops relative to each other (see Ref. [4] and the literature cited therein). Spontaneous thermocapillary migration occurs also due to thermo- and solutohydrodynamic instability of a single drop in the presence of interphase heat or mass transfer or chemical reactions, that result in a breaking of the radial symmetry of the temperature and/or concentration distributions, and induce self-sustained translational drop motion (see Ref. [5] and the literature cited therein). The dynamics of compound drops has attracted the attention of scientists in recent years due to their wide range of applications in many fields of physics, biology, and engineering. Multiphase droplets are encountered in processes such as melting of ice particles in the atmosphere; direct contact heat exchange; and rapid evaporation of drops in a superheated liquid, liquid membranes, and liquid bilayers.

The first thorough analysis of static two-liquid drop configurations was performed by Torza and Mason [6]. They showed that two immiscible drops embedded in a third immiscible fluid, initially in contact, will achieve particular types of configuration: complete engulfment, partial engulfment, or nonengulfment depending solely on the surface tensions between the three pairs of the phases involved. Mahadevan *et al.* [7] studied the statics of compound droplets made of two immiscible fluids on a rigid substrate, in the limit when gravity is dominated by capillarity, and found a richer set of possible configurations. In particular, configurations with four phases merging along a single contact line were shown to occur for a range of interfacial energies and droplet volumes.

Most of the studies of the dynamics of compound two-phase drops with complete and partial engulfment were conducted under the limiting assumption of nondeformable interfaces (i.e., 0 capillary numbers). In practice, the nondeformable case is typical for tiny droplets, while larger fluid particles are substantially deformed by the flow. A comprehensive review of earlier works on the subject can be found in Ref. [8].

A number of works concerning thermocapillary migration of compound drops with complete engulfment are available in the literature as well. The dynamics of concentric compound drops under externally imposed temperature or surfactant

concentration gradient was studied by Borhan *et al.* [9] and Haj Hariri *et al.* [10]. The case of eccentric compound drops was investigated by Morton *et al.* [11]. The motion that results from both a temperature field and residual contaminations applied at the surface of a liquid system was analyzed by Lyell and Carpenter [12]. Tsemakh *et al.* [13] have studied the locomotion of a fully engulfed viscous compound drop, which was induced by an internal secretion of a weak surface-active substance. Their analysis considered also nonlinear effects such as deformation of the interfaces for small capillary numbers using the method of perturbations. Self-propelling of bislugs in capillary tubes [14] is another interesting example of the spontaneous motion of compound drops.

The motion of nearly spherical partially engulfed compound drops with one of the phases forming a thin film on the surface of another one was studied by Sadhal and Johnson [15] making use of the perturbation expansion in terms of small thickness of the film. Oguz [16] and Voung and Sadhal [17] employed the toroidal coordinate system to construct the exact solution for the creeping flow induced by the growth and translation of an axisymmetric liquid-vapor drop or liquid-liquid partially engulfed undeformed compound drop.

A series of studies by Palaniappan, Kim, and Daripa [18–20] is devoted to the special configuration of a partially engulfed compound drop, formed by overlapping spherical segments with a contact angle of $\pi/2$, and with a further assumption that one of the dispersed phases is gaseous (inviscid). These solutions do not satisfy the tangential stress balance at the inner interface separating the two finite domains. The authors argue that this imbalance can be in some cases annihilated by the Marangoni traction with some control mechanism.

A numerical method based on boundary integral equations was developed by Bazhlekov [21] and Bazhlekov *et al.* [22], who present a few model computations. These include the deformation in a shear flow of a two-drop aggregate having initially a static equilibrium shape and the engulfment process starting with an initially nonequilibrium configuration. Recently, Rosenfeld *et al.* [23] used perturbation technique to study the stationary deformation of a partially engulfed compound drop falling in a viscous fluid under the effect of gravity.

Despite its great importance, the subject of thermocapillary migration of a partially engulfed compound drop was not investigated until recently. Rosenfeld *et al.* [24] employed toroidal coordinates and examined the motion of a partially engulfed compound drop induced by the Marangoni effect due to an imposed linear temperature field. The particular case studied there was limited by the assumption of equal thermal conductivities of all three phases and hence in that case the temperature field remained unperturbed. Later, Rosenfeld *et al.* [25] extended these studies to the cases of different thermal conductivities of the phases and to the spontaneous thermocapillary induced motion, with the surface tension gradients resulting from the interfacial heat transfer and the geometric nonuniformity of the system.

It was found that, typically, the motion of a partially engulfed compound drop is induced in the direction of the temperature gradient similar to the case of a single-phase droplet. Nevertheless, it was demonstrated that some interesting cases exist, in which the hybrid drop moved against the temperature gradient. Such behavior was observed in certain ranges of the volume ratio of the drop phases and the associated phases contact angles when the motion was driven mostly by surface tension gradients at the inner interface of the compound drop.

The goal of the present work is to study the physical evolution of the shape of partially engulfed compound drops undergoing thermocapillary migration in a linear temperature field. The paper is organized as follows: Below, in Sec. II, we analyze characteristic time scales and governing parameters of the problem, formulate the mathematical model, and briefly describe the method of solution. Possible scenarios of compound-drop shape evolution are described in Sec. II as well. Several examples of dynamic evolution of the drop's shape due to thermocapillary forcing are presented in Sec. III. The paper closes with a summary of the main results and a discussion of their possible generalization in Sec. IV.

II. STATEMENT OF THE PROBLEM

Consider a partially engulfed compound fluid drop embedded in a nonisothermal viscous medium (fluid 2), with the phases being immiscible. The compound drop consists of two phases (fluids 1 and 3) and possesses three fluid-fluid interfaces, Γ_{ij}, that intersect at a three-fluid contact line. In its equilibrium configuration, the compound drop comprises three spherical surface segments, intersecting at contact angles, which are determined by the force balance at the triple junction [6]:

$$\cos\theta_i = \left(\hat{\gamma}_{jk}^2 - \hat{\gamma}_{ij}^2 - \hat{\gamma}_{ik}^2\right)/(2\hat{\gamma}_{ij}\hat{\gamma}_{ik}), \qquad \theta_i \in (0,\pi). \quad (1)$$

In this article we do not employ indicial summation. Subscripts designate relations to phases or interfaces. Thus, i is the number of the phase corresponding to angle θ_i (see Fig. 1) and $\hat{\gamma}_{mn}$ denotes the interfacial tensions between phases m and n. Note that the nondeformed shape possesses an axial symmetry. A schematic description of a partially engulfed compound drop is depicted in Fig. 1.

We consider, henceforth, a nonisothermal environment with the temperature variation along the interfaces induced by an externally imposed linear field with a constant gradient, $\nabla\hat{T}$, collinear to the axis of the drop. The nonuniform interfacial

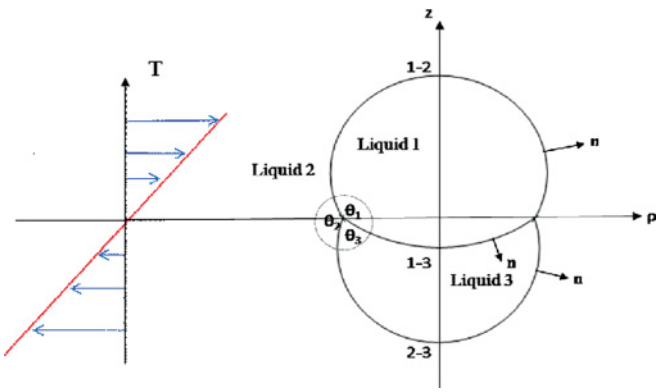

FIG. 1. Configuration of a partially engulfed fluid-fluid compound drop.

tension results in an axisymmetric thermocapillary flow and a net migration of the drop.

The interfacial tensions $\hat{\gamma}_{ij}$ are, in general, functions of the thermodynamic state variables. In this work we assume that the temperature variations along each interface are not large and that

$$\hat{\gamma}_{ij} = \hat{\gamma}_{ij}(\hat{T}) = \hat{\gamma}_{ij}(\hat{T}_0) - \hat{\gamma}_{ij}^T(\hat{T}_0)(\hat{T} - \hat{T}_0), \tag{2}$$

where $\hat{T}$ is the local temperature and $\hat{T}_0$ is the temperature at the three-phase contact line. Normally, interfacial tension decreases with temperature and the rates of change of $\hat{\gamma}_{ij}$ with temperature, $\hat{\gamma}_{ij}^T$, are positive.

We render the length, velocity, stream function, stress, temperature, and interfacial tensions nondimensional using R^*, U^*, $R^{*2}U^*$, $\mu_2 U^*/R^*$, $R^*|\nabla\hat{T}|$, and $\hat{\gamma}^* = \hat{\gamma}_{12}^0(\hat{T}_0|_{t=0})$, respectively. Here R^* is the radius of a sphere having a volume equal to the volume of the compound drop, μ_i denotes the viscosity of phase i, and U^* (following Young *et al.* [1]) is a velocity proportional to that of the thermocapillary migration velocity of a spherical drop of radius R^* submerged in fluid 2, $U^* = \hat{\gamma}_*^T R^*|\nabla\hat{T}|/\mu_2$, with $\hat{\gamma}_*^T$ being some characteristic value of temperature derivative of surface tension. The Reynolds number associated with the problem $\mathrm{Re} = U^* R^*/\mu_2$, is typically of the order 10^{-4} or less. Consequently, in this paper we consider it negligibly small and adopt a quasistationary creeping flow approximation. Thus, the bulk flow is governed by the Stokes equations that have the form:

$$\begin{gathered}\nabla\cdot\mathbf{u} = 0, \quad \nabla\cdot\boldsymbol{\sigma} = 0\,, \\ \boldsymbol{\sigma} = -p\mathbf{I} + \lambda_i(\nabla\mathbf{u} + \nabla\mathbf{u}^T), \quad \mathbf{x}\in\Omega_i,\end{gathered} \tag{3}$$

where Ω_i denotes the domain occupied by fluid i, while $\mathbf{u}$, p, and $\boldsymbol{\sigma}$ are the velocity, dynamic pressure, and stress fields in the respective domains with $\lambda_i = \mu_i/\mu_2$. The scaled interfacial tensions are $\gamma_{ij}(T) = \gamma_{ij}^0 - \frac{\hat{\gamma}_{ij}^T}{\hat{\gamma}^*}R^*|\nabla\hat{T}|T$, with $\gamma_{ij}^0 = \hat{\gamma}_{ij}(\hat{T}_0)/\hat{\gamma}^*$ and $T = (\hat{T} - \hat{T}_0)/(R^*|\nabla\hat{T}|)$. Additional governing parameters of the problem are the capillary number, $\mathrm{Ca} = \mathrm{Ca}_{12} = \mu_2 U^*/\hat{\gamma}^* = \hat{\gamma}_*^T R^*|\nabla\hat{T}|/\hat{\gamma}^*$, and the ratios $\hat{\gamma}_i^T/\hat{\gamma}_*^T$ that are addressed below as the relative thermal activities of the interfaces. Capillary number varies from vanishingly small to order 1. In the present study we concentrate on the case $\mathrm{Ca} \ll 1$. In terms of these parameters the scaled interfacial tensions are

$$\gamma_{ij} = \gamma_{ij}(T) = \gamma_{ij}^0 - \frac{\hat{\gamma}_{ij}^T}{\hat{\gamma}_*^T}\,\mathrm{Ca}\,T. \tag{4}$$

The interfacial conditions are the continuity of the velocity field,

$$[\mathbf{u}] = 0\,, \quad \mathbf{x}\in\Gamma_{ij}\,, \quad i = 1,2\,, \quad j = 2,3\,, \quad i\neq j, \tag{5}$$

and the stress balance,

$$\begin{gathered}[\boldsymbol{\sigma}]\cdot\mathbf{n} = \left(\frac{\gamma_{ij}}{\mathrm{Ca}}\right)(\nabla\cdot\mathbf{n})\,\mathbf{n} - \frac{1}{\mathrm{Ca}}\nabla_S\gamma_{ij}, \\ \mathbf{x}\in\Gamma_{ij}, \quad i = 1,2, \quad j = 2,3, \quad i\neq j,\end{gathered} \tag{6}$$

where $\mathbf{n}$ denotes a unit outer normal and $\nabla_S = \nabla - (\nabla\cdot\mathbf{n})\mathbf{n}$ is a surface gradient at the corresponding surface. Here and below [] denotes the jump across each surface of the drop from the outside to the inside. Projections of Eq. (6) to normal and tangential directions, respectively, are (for axisymmetric surfaces that are considered in the present work)

$$\begin{gathered}[\boldsymbol{\sigma}] : \mathbf{nn} = \left(\frac{\gamma_{ij}}{\mathrm{Ca}}\right)(\nabla\cdot\mathbf{n})\,, \\ \mathbf{x}\in\Gamma_{ij}, \quad i = 1,2, \quad j = 2,3, \quad i\neq j,\end{gathered} \tag{7}$$

and, making use of Eq. (4),

$$[\boldsymbol{\sigma}] : \mathbf{ns} = \frac{\hat{\gamma}_{ij}^T}{\hat{\gamma}_*^T}\frac{\partial T}{\partial s}\,, \quad \mathbf{x}\in\Gamma_{ij}, \quad i = 1,2, \quad j = 2,3, \quad i\neq j, \tag{8}$$

with $\mathbf{s}$ being a unit tangent vector to the interface.

Note that, for the problem under consideration, the time scales for the net motion of the compound drop and for the deformation of its surfaces are $t^* = R/U^*$ and $t_S = \Delta R\,\mu_2/\gamma_{12} = \mathrm{Ca}\Delta R/Rt^*$, respectively, with ΔR being a characteristic deviation from the equilibrium shape. These are always larger than the one associated with the conformation of the viscous flow to any intermediate shape, $t_F = \mathrm{Re}t^*$, since the latter is proportional to the Reynolds number which is vanishingly small.

A deformation of the interfaces of the compound drop can result from three processes. The basic shape may be altered and the spherical segment interfaces can evolve mainly following changes in the three-phase contact angles. In addition, the various interfaces can deform to deviate from their basic spherical segment shapes due to the tension variation on them and due to the flow-induced stresses. It follows from Eq. (7) that, at the leading order in small Ca, the compound drop interfaces may be considered nondeformable at each time step as well as at times of the order t^*. However, in contrast to the case of a single-phase drop, at times of the order t^*/Ca a considerable change in the two-phase partially engulfed drop configuration can take place even when tension and flow-driven deformation are small. Thus, studying the former kind of shape evolution of an, otherwise, "nondeformable compound drop" is the main subject of this paper. As is shown in the following section, in some cases a critical change of the topology of the aggregate may occur, resulting in either a separation of the compound object into two single-phase drops or a complete engulfment of one of the drop immiscible parts by the other.

It was mentioned above that the resulting shape of the compound drop is determined by the contact angles θ_i, related to the interfacial tensions by Eq. (1). Since the interfacial tensions depend on the temperature at the three-phase contact line, they will change with the propagation of the drop to the hotter (or cooler) regions of the ambient medium.

The formulations of the problem should be completed by the heat equation and corresponding boundary conditions. In order to isolate the effect of shape evolution and to avoid computations of the bulk thermal fields, we follow Rosenfeld *et al.* [23] and restrict our study to the case of equal thermal conductivities of all three phases, where, in the absence of significant convective effects, the temperature field remains unperturbed. The generalization to the case of arbitrary heat conductivities is straightforward.

Choose a coordinate system with the z axis collinear to the temperature gradient and the axis of the drop, with the three-phase contact line located initially at the $z = 0$ plane. Let $\hat{T}_0 = \hat{T}|_{\hat{z}=0}$. Then, in scaled variables, $T = z$ and, hence, the interfacial tensions and the contact angles are the functions of z as well, with Z_C being the position of the three-phase contact line

$$\gamma_{ij} = \gamma_{ij}(z) = \gamma^0_{ij} - \hat{\gamma}^T_{ij}/\hat{\gamma}^T_* \,\mathrm{Ca}\, z$$
$$= \gamma_{ij}[Z_C(t)] - \hat{\gamma}^T_{ij}/\hat{\gamma}^T_* \,\mathrm{Ca}\,[z - Z_C(t)]. \qquad (9)$$

Each interface can be considered as nondeformable if the first term in the right-hand-side of Eq. (9) is much larger than the second one. Since at each interface $z - Z_C(t) = O(1)$ and $\mathrm{Ca} \ll 1$, this condition holds as long as $\gamma_{ij}[Z_C(t)] = O(1)$. In scaled variables, the velocity of the drop is of the order 1. Hence, during the time of $O(1)$, the expected deviation from the initial shape is small, of $O(\mathrm{Ca})$. However, with the passage of time of $O(1/\mathrm{Ca})$ the drop moves to the distance of $O(1/\mathrm{Ca})$ and the contact angles and the shape of the drop are expected to change significantly, while the assumption of nondeformability of the drop is still valid. In the present work we are interested in the behavior of the compound drop in a time scale of $O(1/\mathrm{Ca})$, when the drop is much smaller than the distance it travels. The velocity of the compound drop at any moment can be calculated, to the leading order, as the velocity of the nondeformable drop with contact angles computed according to Eq. (1) with $\gamma_{ij} = \gamma_{ij}[Z_C(t)]$. The velocity calculations were performed making use of the presentation of the general solution for the Stokes stream function in toroidal coordinates [26] following Rosenfeld *et al.* [23].

Recall that two immiscible fluids, 1 and 3, embedded in a third immiscible fluid, 2, can achieve four types of configurations [6]: complete engulfment of phase 3 by phase 1, complete engulfment of phase 1 by phase 3, partial engulfment, or nonengulfment. It follows from Eq. (1) that the particular type of configuration depends solely on the ratios of surface tensions between the three pairs of the phases involved, two of which are independent parameters.

A phase diagram of possible configurations of two immiscible drops at the $(\gamma_{12}/\gamma_{13}, \gamma_{23}/\gamma_{13})$ plane is presented in Fig. 2. Domains A, B, C, and D separated by solid lines correspond to the following configurations: phase 3 inside phase 1, partial engulfment, phase 1 inside phase 3, and separated drops, respectively.

If a compound drop, initially of the partially engulfed configuration corresponding to some point in the domain B, undergoes thermocapillary migration, it propagates in the temperature field and the ratios of interfacial tensions continuously change. Thus, each case of the drop dynamics can be reflected by a curve at the phase plane, parametrized by T. Obviously, four different scenarios of the drop behavior are possible:

(I) The curve intersects the boundary of domain B and comes to domain A. Phase 1 completely engulfs phase 3.

(II) The curve intersects the boundary of domain B and comes to domain D. The two-phase drop splits into two single-phase ones.

(III) The curve intersects the boundary of domain B and comes to domain C. Phase 3 completely engulfs phase 1.

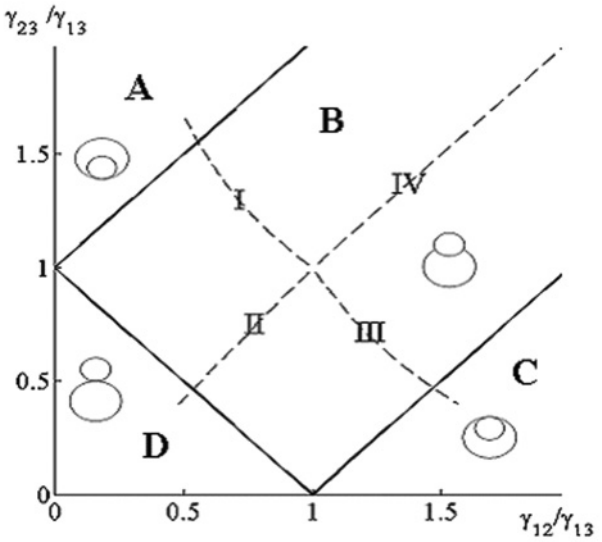

FIG. 2. Phase diagram of possible configurations of two immiscible drops and possible scenarios of their dynamic change with interfacial tension ratios. A, phase 1 engulfed by phase 3; B, partial engulfment; C, phase 3 engulfed by phase 1; D, separation. Marked lines are possible scenarios of the evolution of the partially engulfed drop. I, phase 3 engulfed by phase 1; II, the drop's immiscible parts separate; III, phase 1 engulfed by phase 3; IV, the drop remains partially engulfed.

(IV) The curve does not intersect the boundary of domain B. The drop keeps the partially engulfed configuration.

These scenarios are illustrated in Fig. 2 by correspondingly marked dashed lines.

III. EXAMPLES OF THE DYNMAMIC EVOLUTION OF A NONDEFORMABLE COMPOUND DROP

Rosenfeld *et al.* [23,24] computed the thermocapillary induced velocity of a partially engulfed compound drop of various given shapes and various dependencies of the interfacial tensions on the temperature. It was demonstrated that, normally, the motion of a drop is induced in the direction of the temperature gradient similar to the case of a single-phase droplet. However, some cases in which the hybrid drop moved against the temperature gradient were observed as well. Since for cases in which the motion is in the direction of the temperature gradient the interfacial tensions typically decrease, whereas for cases where the motion is in the opposite direction they grow, one can anticipate quite different behavior patterns of the aggregate. We consider these cases separately in Secs. III A and III B, respectively.

To illustrate the effect of interfacial tension variation on the dynamic change of shape of a partially engulfed compound drop, we consider drops to have initially the same shape but different linear dependencies of surface tensions on the temperature, leading to entirely different scenarios of drop evolution. For the common initial shape, we chose the one with contact angles $\theta_1 = 0.8722\pi$, $\theta_2 = 0.95\pi$, and $\theta_3 = 0.1778\pi$, resulting from the specific surface tension values $\hat{\gamma}_{12} = 0.061 N/m$, $\hat{\gamma}_{13} = 0.018 N/m$, and $\hat{\gamma}_{23} = 0.045 N/m$,

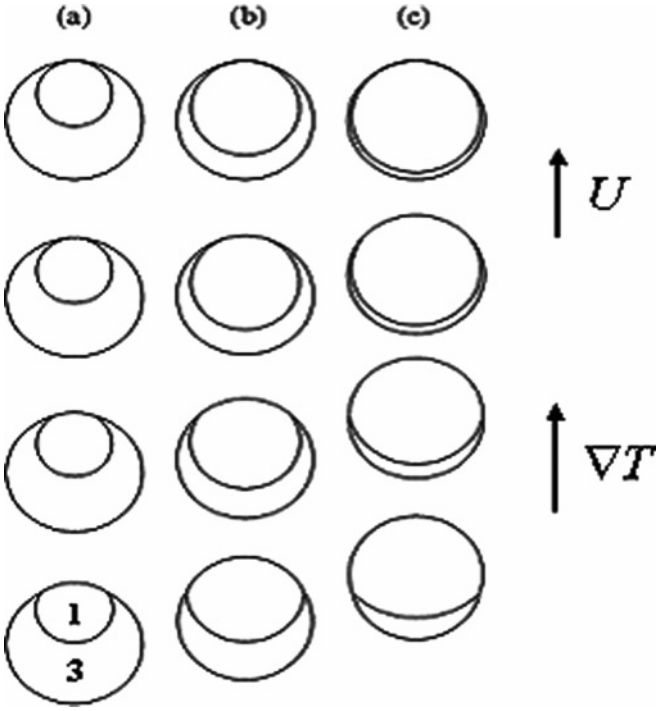

FIG. 3. The shape evolution for a partially engulfed compound drop undergoing thermocapillary migration in the direction of the temperature gradient (upward) with (a) $V_1/V_3 = 0.2$, (b) $V_1/V_3 = 1$, and (c) $V_1/V_3 = 5$. $\gamma_{12} = 1 - 0.1\mathrm{Ca}\,T$, $\gamma_{13} = 0.2952 - 0.1\mathrm{Ca}\,T$, $\gamma_{23} = 0.7374 - 0.1\mathrm{Ca}\,T$. The vertical positions of Z_C from bottom to top are at 0, 0.26/Ca, 0.32/Ca, and 0.326/Ca. Eventually, phase 1 is engulfed by phase 3.

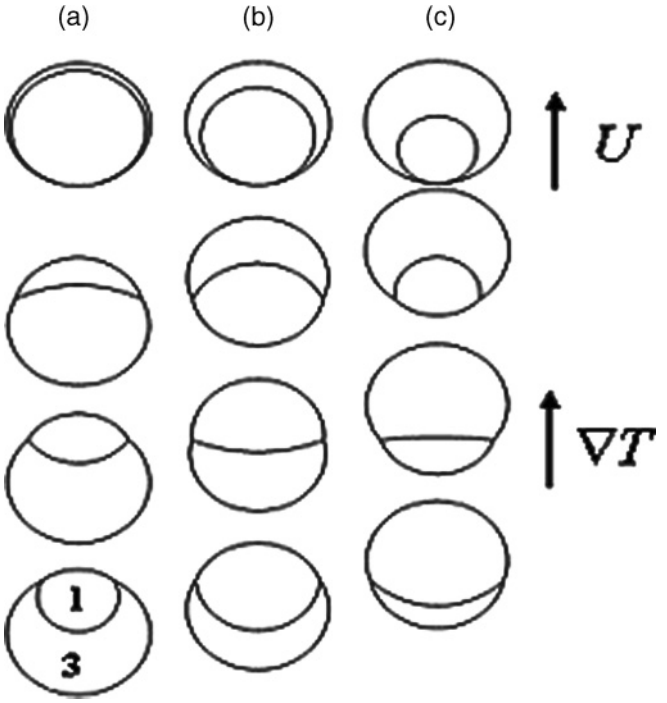

FIG. 4. The shape evolution for a partially engulfed compound drop undergoing termocapillary migration in the direction of the temperature gradient (upward) with $\gamma_{12} = 1 - 0.4\mathrm{Ca}\,T$, $\gamma_{13} = 0.2952 - 0.1\mathrm{Ca}\,T$, and $\gamma_{23} = 0.7374 - 0.1\mathrm{Ca}T$. (a) $V_1/V_3 = 0.2$. (b) $V_1/V_3 = 1$. (c) $V_1/V_3 = 5$. The vertical positions of Z_C from bottom to top are at 0, 0.6/Ca, 1.3/Ca, and 0.136/Ca, respectively. Eventually, phase 3 is completely engulfed by phase 1.

quoted by Vuong and Sadhal [17] and used as base examples also in Refs. [23,24].

A. Migration in the direction of the temperature gradient

Various scenarios of the shape evolution for compound drops migrating in the direction of the temperature gradient are presented in Figs. 3–6. The three-phase contact line of the shapes at each row in these figures corresponds to a specific vertical position, Z_C, while columns (a), (b), and (c) correspond to volume ratios, V_1/V_3, of 0.2, 1, and 5, respectively. Figure 3 illustrates the dynamics of compound drops with equal thermal activities of the interfaces, i.e., interfacial tensions at all three interfaces having equal derivatives with respect to temperature,

$$\gamma_{12} = 1 - 0.1\,\mathrm{Ca}\,T, \quad \gamma_{13} = 0.2952 - 0.1\,\mathrm{Ca}\,T, \quad \gamma_{23} = 0.7374 - 0.1\,\mathrm{Ca}\,T. \tag{10}$$

The drop attains a velocity in the direction of the applied temperature gradient and migrates upward. Since the initial values of surface tensions are different, their ratios change with time and lead to the change in the shape of the aggregate according to Eq. (1). In this case, the ratios γ_{13}/γ_{12} and γ_{23}/γ_{12} decrease while the tension at Γ_{12} becomes relatively stronger. As a result, the surface Γ_{12} constantly shrinks and eventually this interface vanishes. At this instant the balance of the horizontal components of the force at the three-phase contact line can no longer be maintained and, as a result, phase 1 becomes entirely engulfed by phase 3, i.e., scenario III takes place. In Fig. 3, the Γ_{12} positions of the three-phase contact line for each row are 0, 0.26/Ca, 0.32/Ca, and 0.326/Ca, respectively.

A different and opposite scenario I is illustrated in Fig. 4. Here, the thermal activity of the interface 1–2 is 4 times higher than the others,

$$\gamma_{12} = 1 - 0.4\,\mathrm{Ca}\,T, \quad \gamma_{13} = 0.2952 - 0.1\,\mathrm{Ca}\,T, \quad \gamma_{23} = 0.7374 - 0.1\,\mathrm{Ca}\,T. \tag{11}$$

The positions of the 3-phase contact line for each row are 0, 0.6/Ca, 1.3/Ca, and 1.36/Ca, respectively. In this case, the ratio γ_{13}/γ_{12} increases, while γ_{23}/γ_{12} decreases, and, thus, the tension at Γ_{23} becomes relatively stronger. This interface shrinks and eventually disappears. Phase 3 becomes entirely engulfed by phase 1.

Yet another scenario II is presented in Fig. 5, where the interface separating the drop phases is thermally inactive,

$$\gamma_{12} = 1 - 0.1\,\mathrm{Ca}\,T, \quad \gamma_{13} = 0.2952, \quad \gamma_{23} = 0.7374 - 0.1\,\mathrm{Ca}\,T. \tag{12}$$

The positions of the contact lines for each row are 0, 5/Ca, 7/Ca, and 7.21/Ca, respectively. Since, in this case, the inner interface 1–3 is not thermally active, its tension does not change with the propagation of the drop, while the surface tensions at the outer interfaces decrease. As a result the tension

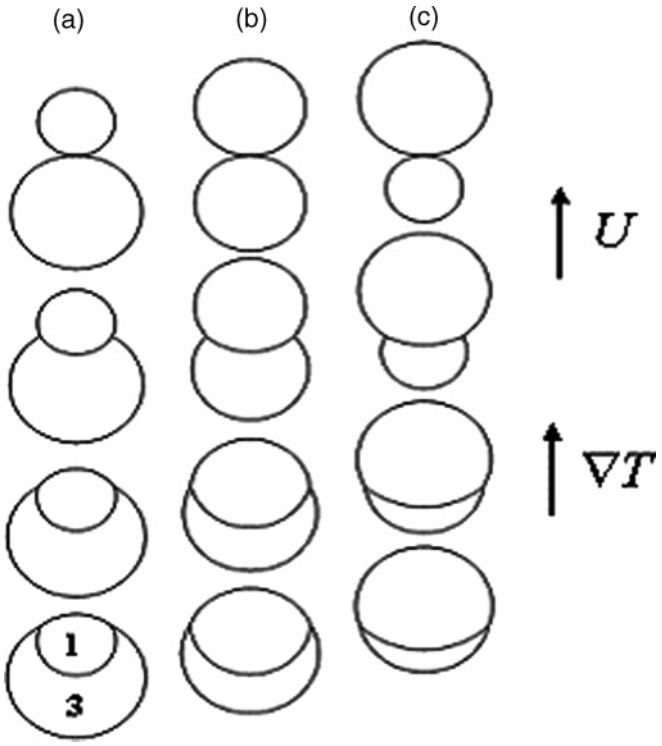

FIG. 5. The shape evolution for a partially engulfed compound drop undergoing thermocapillary migration in the direction of the temperature gradient (upward) with $\gamma_{12} = 1 - 0.1\mathrm{Ca}T$, $\gamma_{13} = 0.2952$, and $\gamma_{23} = 0.7374 - 0.1\,\mathrm{Ca}T$. (a) $V_1/V_3 = 0.2$. (b) $V_1/V_3 = 1$. (c) $V_1/V_3 = 5$. The vertical positions of Z_C from bottom to top are at 0, 5/Ca, 7/Ca, and 7.21/Ca, respectively. Eventually, drop parts 1 and 3 separate.

at Γ_{13} becomes relatively stronger, this interface shrinks with the drop progress and eventually disappears. The immiscible parts of the compound drop separate.

The three scenarios described above lead to different changes in the topology of the compound object, although the initial configuration is the same. Note that such changes do not take place (scenario IV) if the ratios of interfacial tensions change very slowly or do not change at all, as in the case

$$\gamma_{12} = 1 - 0.1T/\mathrm{Ca}, \quad \gamma_{13} = 0.2952 - 0.02952\,\mathrm{Ca}\,T, \quad \gamma_{23} = 0.7374 - 0.07374\,\mathrm{Ca}\,T. \tag{13}$$

As it was demonstrated, the qualitative type of the evolution of the compound object is determined solely by the temperature dependence of the interfacial tensions involved and is independent of the volumes and viscosities of the phases. These parameters, however, strongly affect the dynamics of the process in time. To study this dynamics we calculated quasistationary thermocapillary migration velocities of the compound drop as functions of the contact line positions for the cases depicted in Figs. 3–5 for various values of viscosity ratio.

The velocity was computed making use of the general solution for the Stokes stream function in toroidal coordinates as in Refs. [17] and [26]. The coefficients entering this general solution were determined following the procedure developed in Ref. [23]. The results of the velocity calculation are presented in Fig. 6. Figures 6(a) and 6(b), Figs. 6(c) and 6(d), and Figs. 6(e) and 6(f) are computed for surface tensions given by Eqs. (10), (11), and (12), respectively.

Figures 6(a), 6(c), and 6(e) illustrate the dependence of the migration velocities on the phases' volume ratio. Dashed, dotted, and solid curves in these figures are computed for $V_1/V_3 = 0.2$, 1, and 6, corresponding to the left, middle, and right columns in Figs. 3–5, respectively. In Figs. 6(a) and 6(b) one can see that the migration velocities decrease as the phase 1 velocity becomes more and more engulfed by phase 3 and attains some positive values at the limiting entirely engulfed configurations. The migration velocities decrease with the growth of the volume ratio V_1/V_3 and almost vanishes at the limiting thin shell configuration at $V_1/V_3 = 5$ as is obvious in Fig. 6(a). Both phenomena are due to the increase of the Stokes drag and to the retarding effect of the Marangoni traction at the inner interface Γ_{13}, as found in Ref. [23]. In the cases depicted in Fig. 6(a), this interface constantly grows with the propagation of the drop and the retardation effect becomes more significant.

In Fig. 6(b) one can see that the migration velocities decrease with the growth of the viscosity of the drop. However, this dependence is weaker for configurations that are close to the limiting one with the complete engulfment of phase 1.

Figures 6(c) and 6(d) illustrate the case resulting in the total engulfment of phase 3 by phase 1, with thermal activity of the interface Γ_{12} being 4 times higher than that of the other two (see Fig. 4). The dynamic change of the velocity drastically differs from that in the cases of equal thermal activities of the interfaces depicted in Fig. 6(a). Here, the surface of the interface Γ_{12} is constantly augmented (see Fig. 5), resulting in the growth of the net Marangoni force exerted on the drop. In the case $V_1/V_3 = 0.2$, this leads to a monotonous growth of the migration velocity, while for the higher volume ratios the increase in the resistance prevails at intermediate stages of the process and the velocity dependence on the position is not monotonic. The dependence of the velocity on the viscosity of phase 1 becomes more pronounced as it engulfs phase 3, as is evident in Fig. 6(d).

Figures 6(e) and 6(f) show the increase of velocity of the compound drop with a thermally nonactive inner interface Γ_{13} during the process, resulting in the separation of the parts of the drop. This phenomenon can be explained by the increase in size of the thermally active surfaces. The dependence on the viscosity of phase 1 becomes more pronounced with the separation of the phases. However, the effect of each parameter on the velocity is, in this case, weaker than in the processes leading to the complete engulfment.

An interesting question is what happens to the drop parts after the separation occurs. Do the parts separate or will the motion continue in the touching drop configuration. Obviously, this behavior depends on the migration velocity that the two drops would attain if separated by a small gap. If the velocity of the leading drop exceeds that of the trailing one they will naturally separate, whereas, in the opposite case, they maintain the touching drops configuration. These velocities can be computed making use of bispherical coordinates following Morton *et al.* [11]. However, some conclusions concerning the cases shown in the Fig. 6 can be made without computations. Thus, it was shown in Morton *et al.* [11] that, if the drops have the same viscosities and surface properties, the larger one

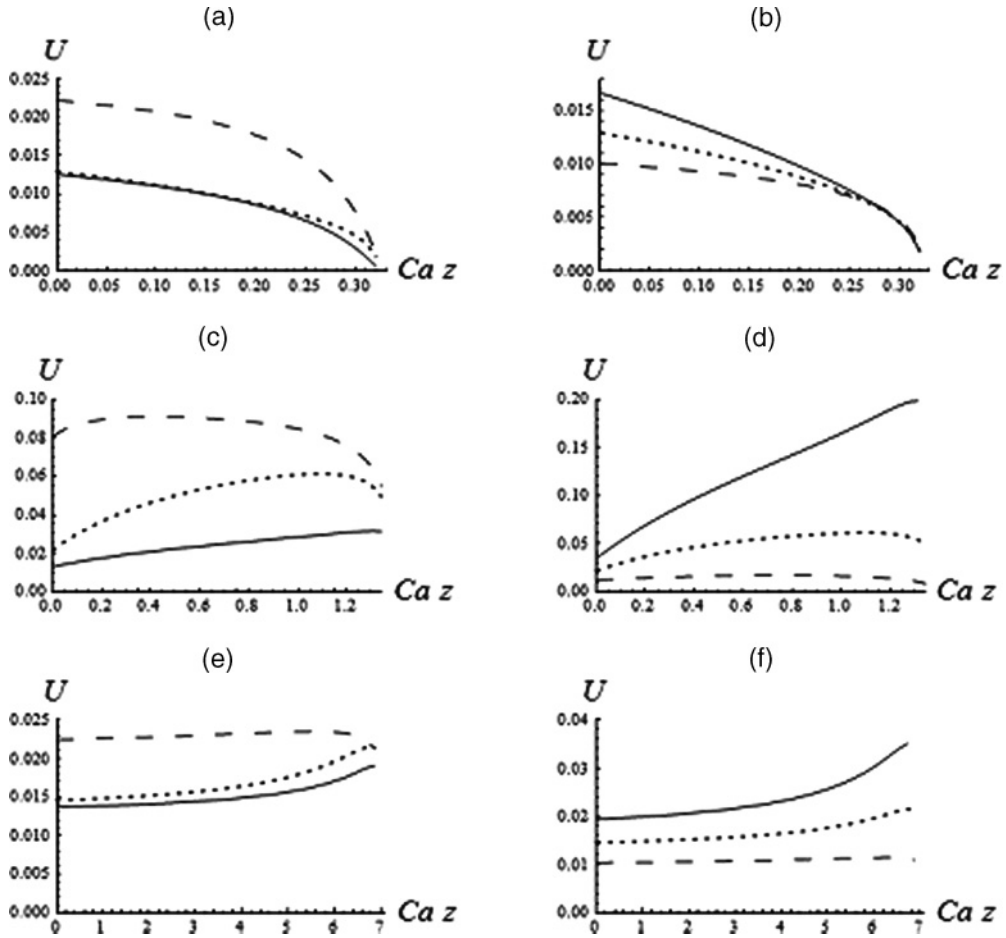

FIG. 6. Thermocapillary migration velocity of a partially engulfed compound drop versus the location of the three-phase contact line. (a) and (b) $\gamma_{12} = 1 - 0.1\mathrm{Ca}\,T, \gamma_{13} = 0.2952 - 0.1\mathrm{Ca}T, \gamma_{23} = 0.7374 - 0.1\mathrm{Ca}T$; (c) and (d) $\gamma_{12} = 1 - 0.4\,\mathrm{Ca}T$, $\gamma_{13} = 0.2952 - 0.1\mathrm{Ca}T, \gamma_{23} = 0.7374 - 0.1\mathrm{Ca}T$; (e) and (f) $\gamma_{13} = 0.2952$, $\gamma_{12} = 1 - 0.1\,\mathrm{Ca}T$, $\gamma_{23} = 0.7374 - 0.1\,\mathrm{Ca}T$. In (a), (c), and (e), $\lambda_1 = \lambda_3 = 1$ and $V_1/V_3 = 0.2$, 1, and 5 for solid, dotted, and dashed lines, respectively. In (b), (d), and (f) $V_1/V_3 = 1$, $\lambda_3 = 1$, and $\lambda_1 = 0.1$, 1, and 10 for solid, dotted, and dashed lines, respectively.

moves faster. Hence, in the case of equal or close viscosities of the drop parts, it is anticipated that the process illustrated in Fig. 5(c) will continue to a separation of the drops, while in the other two cases the motion will continue as an aggregate of touching drops (under the assumption of axial symmetry). Furthermore, when the two daughter drops are of equal size, the one with a lower viscosity moves faster and, hence, the drops depicted in Fig. 5(b) will separate if $\lambda_1 < \lambda_3$ and will preserve a touching drops configuration in the opposite case. Note, however, that the cases where the trailing drop moves faster than the leading one if separated are expected to be unstable with respect to nonaxisymmetric disturbances.

B. Anomalous migration in the direction opposite to the temperature gradient

The computations of Refs. [24,25] revealed that a partially engulfed compound drop can move in a direction opposite to the temperature gradient in cases where the temperature dependence of the surface tension at the inner interface 1-3 is much stronger than that at the outer interfaces. To isolate the effect we consider first the case where only the inner interface is thermally active, while the surface tensions at the outer interfaces do not change with the temperature. Here we chose $U^* = \hat{\gamma}_{13}^T R^* |\nabla \hat{T}|/\mu_2$ for the characteristic velocity.

Figure 7 shows the thermocapillary migration velocities of various compound drops with $\lambda_1 = \lambda_3 = 1$, $\gamma_{12} = 1$, $\gamma_{13} = 0.2952 - \mathrm{Ca}T$, and $\gamma_{23} = 0.7374$ as functions of the three-phase contact line positions. The time dependence of these positions can be easily obtained by integrating the equation $dZ_C/dt = U(Z_C)$. Solid, dashed, dashed-dotted, and dashed lines are calculated for the volume ratios $V_3/V_1 = 9$, 5, 3, and 2, respectively. Since the velocity is negative, the drop moves in the direction opposite to the temperature gradient toward negative z.

In Fig. 7(a) all four cases are plotted using the same scale. One can see that the magnitude of the velocity decreases with the growth of the volume ratio and seems to monotonically decay with the propagation of the aggregate to cooler regions. More accurate analysis [see Figs. 7(b)–7(d)] revealed, however, that only for $V_3/V_1 = 2$ (dashed line) is the migration velocity monotonic, while for the higher volume ratios the velocity achieves several extrema including a zero maximum at some locations.

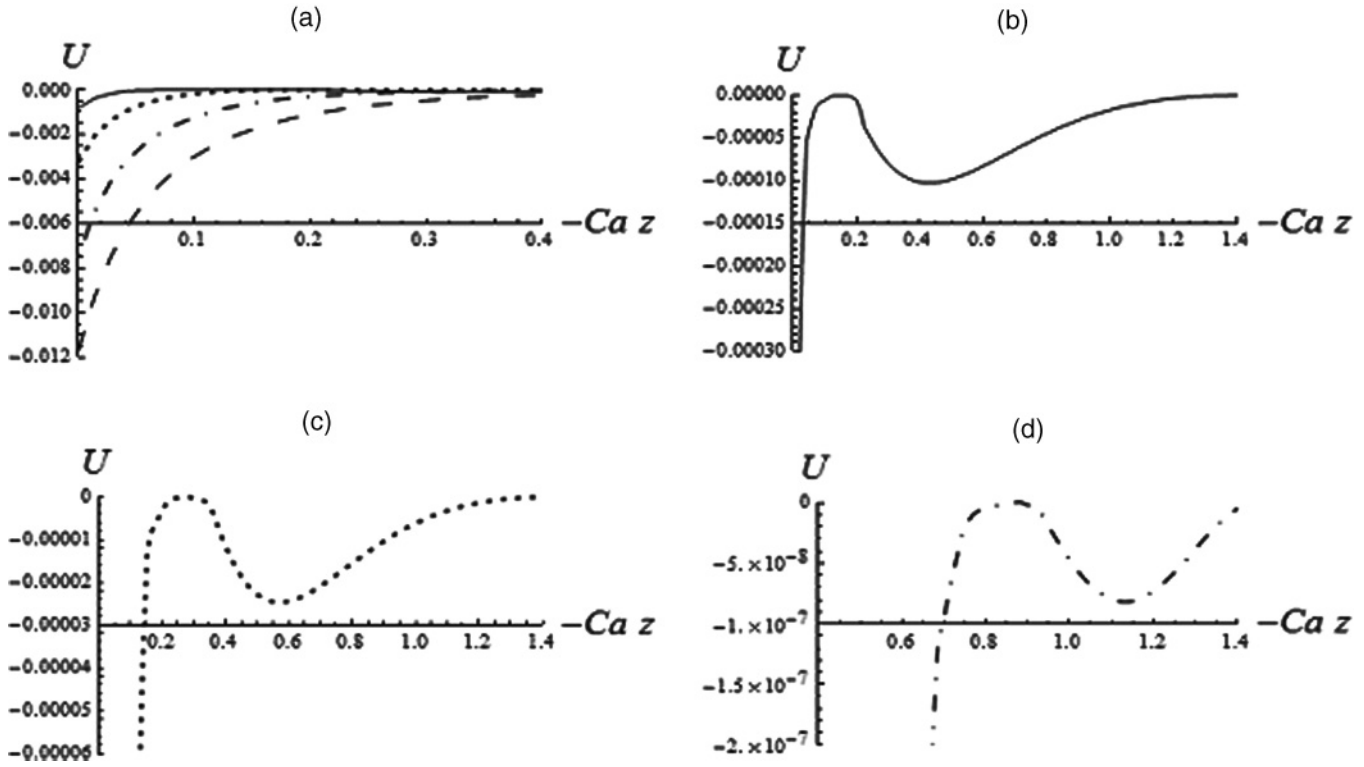

FIG. 7. Thermocapillary migration velocity of a partially engulfed compound drop versus the location of the three-phase contact line. $\gamma_{12} = 1$, $\gamma_{13} = 0.2952 - \mathrm{Ca}T$, $\gamma_{23} = 0.7374$, $\lambda_1 = \lambda_3 = 1$. Solid, dotted, dashed-dotted, and dashed lines are computed for $V_1/V_3 = 9$, 5, 3, and 2, respectively.

The shapes of the drops with interfacial tensions $\gamma_{12} = 1$, $\gamma_{13} = 0.2952 - \mathrm{Ca}T$, and $\gamma_{23} = 0.7374$ and volume ratios $V_3/V_1 = 2$, 3, 5, and 9 at various positions of the three-phase contact line are demonstrated in Figs. 8(a)–8(d), respectively. The migration velocity is negative, and the drops migrate downward. The upper row in Fig. 8 shows the initial configurations at $Z_C = 0$. The second row in Fig. 8 presents the shapes at $Z_C = -0.05/\mathrm{Ca}$. The third and the fourth shapes in Fig. 8(a) are calculated for $Z_C = -0.2/\mathrm{Ca}$ and $-0.8/\mathrm{Ca}$, respectively, while in Figs. 8(b)–8(d) these shapes correspond to positions where the migration velocity is 0 and to a following local minimum of the velocity [see Figs. 7(b)–7(d)]. The lowest row of shapes in Fig. 8 corresponds to the touching drops configurations at $Z_C = -1.422/\mathrm{Ca}$.

It is evident from Figs. 7 and 8 that the migration velocity vanishes for the shapes with flat inner interface. This is not a surprise since, at such configurations, surface tension is constant along each of the interfaces, including the thermally active one, and there is no reason for a thermocapillary flow to exist. In such stationary states all the fluids are quiescent as none of the interfaces exerts any shear on the bulk phases. At this equilibrium position the drop would not move. However, these equilibrium positions are not stable. Indeed, any small shift downward will result in a negative migration velocity, and the drop will proceed slowly moving in the direction opposite to the temperature gradient until the inner interface vanishes completely and, as a result, the drop parts separate. At these limiting configurations again, since the thermally active interface disappeared, all the interfacial tensions are constant and no thermocapillary flow takes place.

Another interesting question is if the drop, initially located above the equilibrium point, can reach it in finite time. The answer is negative. In view of the maxima show in Fig. 7, The migration velocity of the drop located in the vicinity of the equilibrium position, Z_{eq}, can be approximated by $U = dZ_C/dt = -a\,(Z_C - Z_{\mathrm{eq}})^2$, with a being a positive constant. Integrating this equation yields

$$Z_C(t) = Z_{\mathrm{eq}} + \frac{1}{1/(Z_C(0) - Z_{\mathrm{eq}}) + at}.$$

Obviously, if $Z_C\,(0) > Z_{\mathrm{eq}}$, the drop approaches the equilibrium position but reaches it in infinite time. On the other hand, if $Z_C\ (0) < Z_{\mathrm{eq}}$, the drop will move away from the equilibrium with its shape approaching a touching drops configuration. The evolution scenario presented in Figs. 7 and 8 is typical solely for the special case of thermally nonactive outer interfaces of the compound drop. However, even a very weak dependence of the surface tension of one of these interfaces on temperature may drastically change the behavior of the aggregate. An illustration of this change is given in Figs. 9 and 10, where

$$\gamma_{12} = 1 - 0.005\,\mathrm{Ca}T, \quad \gamma_{13} = 0.2952 - \mathrm{Ca}T, \quad \gamma_{23} = 0.7374 - 0.005\,\mathrm{Ca}T. \tag{14}$$

In Fig. 9 the thermocapillary migration velocities are plotted versus the three-phase contact line positions. Solid, dashed, dashed-dotted, and dashed lines are calculated for the volume ratios $V_3/V_1 = 9$, 5, 3, and 2, respectively. One can see that for $V_3/V_1 = 9$ (solid line) the velocity is positive and, hence,

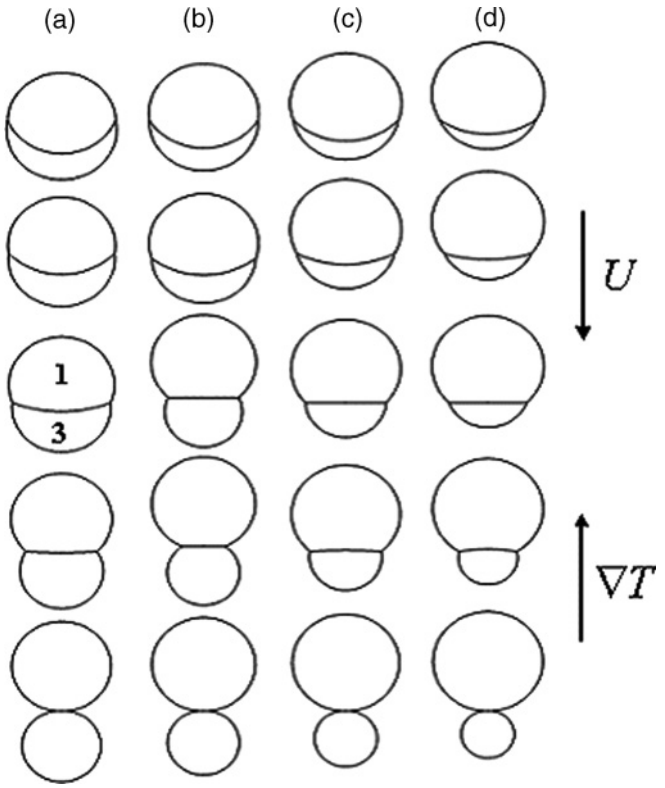

FIG. 8. Dynamic shape evolution of a partially engulfed compound drop undergoing thermocapillary migration in the direction opposite to the temperature gradient. $\gamma_{12} = 1$, $\gamma_{13} = 0.2952 - \mathrm{Ca}T$, $\gamma_{23} = 0.7374$, and $\lambda_1 = \lambda_3 = 1$. $V_1/V_3 =$ 2 (a), 3(b), 5(c), and 9(d). Locations of the three-phase contact line from top to bottom are (a) 0, –0.05/Ca, –0.2/Ca, –0.8/Ca, and –1.422/Ca; (b) 0, –0.05/Ca, –0.9/Ca, –1.15/Ca, and –1.422/Ca; (c) 0, –0.05/Ca, –0.32/Ca, –0.6/Ca, and –1.422/Ca; and (d) 0, –0.05/Ca, –0.17/Ca, –0.4/Ca, and –1.422/Ca.

the drop moves in the direction of the temperature gradient, following one of the scenarios described in the previous section. For smaller volume ratios, the velocity is first negative, then vanishes, and changes sign. The drop moves in the direction opposite to the temperature gradient toward negative z and tends to some equilibrium position, where $U = 0$. In contrast to the previous case, this equilibrium is stable with

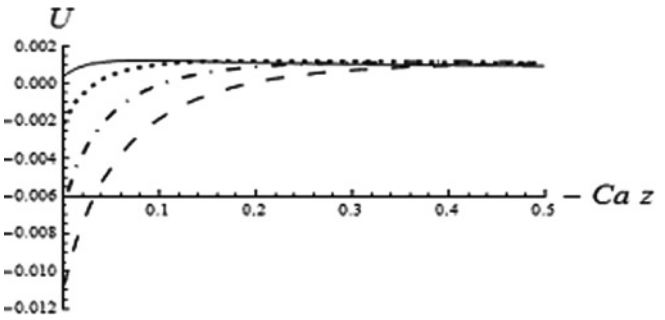

FIG. 9. Thermocapillary migration velocity of a partially engulfed compound drop versus the location of the tree-phase contact line. $\lambda_1 = \lambda_3 = 1$, $\gamma_{12} = 1 - 0.005\,\mathrm{Ca}T$, $\gamma_{13} = 0.2952 - \mathrm{Ca}T$, and $\gamma_{23} = 0.7374 - 0.005\,\mathrm{Ca}T$. Solid, dotted, dashed-dotted, and dashed lines are computed for $V_1/V_3 = 9$, 5, 3, and 2, respectively.

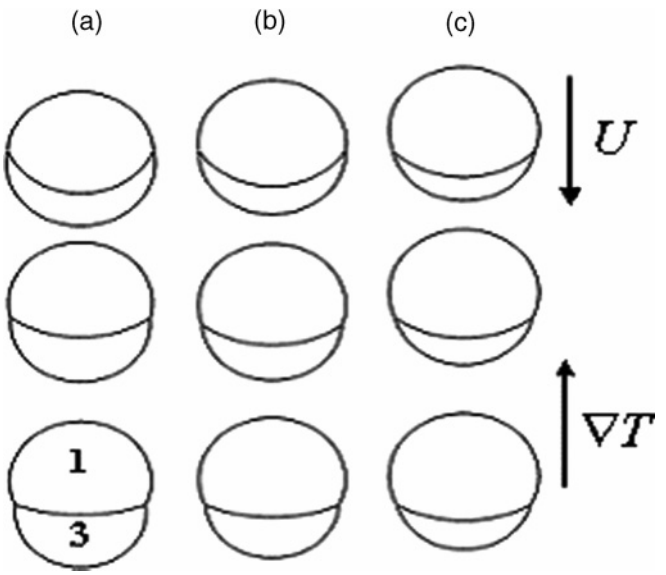

FIG. 10. Dynamic shape evolution of a partially engulfed compound drop undergoing thermocapillary migration in the direction opposite to the temperature gradient. $\lambda_1 = \lambda_3 = 1$, $\gamma_{12} = 1 - 0.005\mathrm{Ca}T$, $\gamma_{13} = 0.2952 - \mathrm{Ca}T$, $\gamma_{23} = 0.7374 - 0.005\mathrm{Ca}T$, and $V_1/V_3 = 2$ (a), 3 (b), and 5 (c). Locations of the three-phase contact line from top to bottom are (a) 0, –0.1/Ca, and –0.24/Ca; (b) 0, –0.05/Ca, and –0.12/Ca; and (c) 0, –0.02/Ca, and –0.04/Ca.

respect to the perturbation of the position of the drop, since any change in the position results in the velocity in the direction of the equilibrium, i.e., the drop shifted downward attains positive velocity, while that shifted upward attains negative velocity. Stability of the equilibrium shape with respect to the perturbations of the interfaces is beyond the scope of this paper. Another difference from the cases illustrated in Figs. 7 and 8 is that the fluids at equilibrium are not quiescent and thermocapillary flow, though rather weak, exists.

At the vicinity of the equilibrium position, Z_{eq}, the migration velocity can be approximated by $U = dZ_C/dt = -a(Z_C - Z_{\mathrm{eq}})$ (see Fig. 9), with a being a positive constant. Integrating this equation yields

$$Z_C(t) = Z_{\mathrm{eq}} + (Z_C(0) - Z_{\mathrm{eq}})e^{-at}.$$

One can see that, in contrast to the previous case, the drop approaches equilibrium position regardless of its initial location being above or below this equilibrium. The approach is faster than in the previous case but, again, it takes infinite time to reach the equilibrium.

The evolution of the shapes of the drops with interfacial tensions (14) and volume ratios $V_3/V_1 = 2$, 3, and 5 is demonstrated in Figs. 10(a)–10(c), respectively. The upper and lower rows show the initial and stable equilibrium configurations, respectively. The middle row corresponds to intermediate configurations. Evidently, the equilibrium configurations are located at much smaller distance from the initial position than in the previous case.

IV. CONCLUSIONS AND DISCUSSION

In this work we studied the dynamic change of the configuration of a fluid-fluid partially engulfed compound

drop undergoing thermocapillary migration in a nonisothermal ambient medium. Under the assumption that the capillary number is small, Ca $\ll$ 1, at each time step the deviation of interfaces of the compound object from spherical segment shapes is negligible. However, as the drop propagates far enough [to a distance of $O(1/\mathrm{Ca})$] through the nonisothermal fluid, the temperature at the three-phase contact line and, hence, the contact angles may considerably change, resulting in a change of the compound drop configuration.

If the drop drifts in the direction of the temperature gradient, the change in the interfacial tension normally results either in separation of the immiscible parts of the compound object or in a complete engulfment of one of the drop phases by the other. The specific scenario depends on the relative rate of change of surface tensions with temperature at the interfaces of the compound object. Generally, the interface with the slowest decrease of its surface tension tends to shrink and eventually vanishes. If this is the inner interface, the two-phase drop splits into two single-phase ones, while in the opposite case complete engulfment takes place. In the special case when the ratios between surface tensions change much slower than these parameters themselves, no topological changes are expected at the distances of $O(1/\mathrm{Ca})$.

The qualitative type of the evolution of the compound object is determined solely by the temperature dependence of the interfacial tensions. However, the dynamics of the process is affected by the volumes and viscosities of the drop phases. In general, the migration velocity decreases with the increase of the viscosity of each of the phases. The dependence on the volume ratio, however, is more complex.

After the separation of compound object parts, the two drops either detach and move apart or they continue migrating in a touching drop aggregate, depending on which daughter drop, leading or trailing, would move faster when separated. The type of behavior after separation is determined by the interplay of all the parameters of the system, except for the surface tension of the inner interface, which disappears.

If the temperature dependence of the surface tension at the inner interface 1-3 is much stronger than that at the outer interfaces, the compound drop can move in the direction opposite to the temperature gradient, i.e., to the cooler regions of the ambient fluid. Since in this case the interfacial tensions grow with the propagation of the aggregate, whereas for the motion in the opposite direction they decrease, the deformation pattern is quite different. If the surface tensions of the outer interfaces are temperature independent, no thermocapillary flow takes place when the compound drop attains a configuration with a flat inner interface as all interfacial tensions become constant. However, the stationary configuration with a flat inner interface is unstable and the evolution proceeds to a complete separation of the drop's immiscible parts, at which point all motions cease again on the surfaces and in the bulks.

Nevertheless, a weak dependence of outer interfaces on temperature drastically changes the limiting behavior of such compound drops. In this case, a stable equilibrium configuration with a curved inner interface is typical. In contrast to the previous case, the compound drop does not move or change its shape at this configuration, but the bulk fluids are not quiescent. Note that the anomalous migration of the compound drop is possible solely in the case when the dependence of interfacial tension on temperature is at least an order of magnitude higher than that at the outer interfaces. For thermocapillary systems such combinations might be quite rare. However, recall the well-known similarity between heat and mass transfer and, therefore, between thermocapillary and solutocapillary effects (see, e.g., Subramanian and Balasubramaniam, [27]). Thus, our results are equally applicable to the Marangoni migration of compound drops in a nonuniform concentration field. The effect of the Marangoni migration in the direction opposite to the concentration gradient is, perhaps, more readily realized when the tension variations are caused by a preferred adsorption of a surface-active substance on the inner interface rather then by temperature variations.

Note finally that, while the linear approximation (2) is well justified for modest temperature variations, the results of this work can be easily generalized to the case of nonlinear dependence of surface tension on the temperature that is typical when the temperature changes considerably.

ACKNOWLEDGMENT

OML acknowledges the support of the Israel Ministry for Immigrant Absorption.

[1] N. O. Young, J. S. Goldstein, and M. J. Block, J. Fluid Mech. **6**, 350 (1959).
[2] Yu. K. Bratukhin, Izv. Akad. Nauk SSSR, Mekh. Zhidk. Gaza **5**, 156 (1975).
[3] R. Balasubramaniam and A. T. Chai, J. Colloid Interface Sci. **119**, 531 (1987).
[4] O. M. Lavrenteva, V. Berejnov, A. M. Leshansky, and A. Nir, Ind. Eng. Chem. Res. **41**, 357 (2002).
[5] M. G. Velarde, A. Y. Rednikov, and Y. S. Ryazantsev, J. Phys.: Condens. Matter **8**, 9233 (1996).
[6] S. Torza and S. G. Mason, J. Colloid Interface Sci. **33**, 67 (1970).
[7] L. Mahadevan, M. Adda-Bedia, and Y. Pomeau, J. Fluid Mech. **467**, 101 (2002).
[8] R. E. Johnson and S. S. Sadhal, Ann. Rev. Fluid Mech. **17**, 286 (1985).
[9] A. Borhan, H. Haj-Hariri, and A. Nadim, J. Colloid Interface Sci. **149**, 553 (1992).
[10] H. Haj-Hariri, A. Nadim, and A. Borhan, J. Fluid Mech. **252**, 265 (1993).
[11] D. S. Morton, R. S. Subramanian, and R. Balasubramaniam, Phys. Fluids A **2**, 2119 (1990).
[12] M. J. Lyell and M. J. Carpenter, Appl. Sci. Res. **14**, 639 (1993).
[13] D. Tsemakh, O. M. Lavrenteva, and A. Nir, Int. J. Multiphase Flow **30**, 1337 (2004).
[14] J. Bico and D. Quere, J. Fluid Mech. **467**, 101 (2002).
[15] S. S. Sadhal and R. E. Johnson, J. Fluid Mech. **126**, 237 (1983).

[16] H. N. Oguz, Ph.D. thesis, University of Southern California, Los Angeles, 1987.
[17] S. T. Vuong and S. S. Sadhal, J. Fluid Mech. **209**, 617 (1989).
[18] D. Palaniappan and S. Kim, Phys. Fluids A **9**, 1218 (1997).
[19] D. Palaniappan and P. Daripa, Phys. Fluids **12**, 2377 (2000).
[20] D. Palaniappan and P. Daripa, Physica A **346**, 217 (2005).
[21] I. B. Bazhlekov, Ph.D. Thesis, Eindhoven, University of Technology, 2003.
[22] I. B. Bazhlekov, P. D. Anderson, and H. E. H. Meijer, Phys. Fluids **16**, 1064 (2004).
[23] L. Rosenfeld, O. M. Lavrenteva, R. Spivak, and A. Nir, Phys. Fluids **23**, 023101 (2011).
[24] L. Rosenfeld, O. M. Lavrenteva, and A. Nir, Phys. Fluids **20**, 072102 (2008).
[25] L. Rosenfeld, O. M. Lavrenteva, and A. Nir, J. Fluid Mech. **626**, 263 (2009).
[26] L. E. Payne and W. h. Pell, J. Fluid Mech. **7**, 529 (1960).
[27] R. S. Subramanian and R. Balasubramaniam, *The Motion of Bubbles and Drops in Reduced Gravity* (Cambridge University Press, Cambridge, UK, 2001).